

# DARPA/AFRL/NASA Smart Wing Second Wind Tunnel Test Results

L. B. Scherer <sup>a</sup>, C. A. Martin <sup>a</sup>, M. West <sup>b</sup>,  
J. P. Florance <sup>c</sup>, C. D. Wieseman <sup>c</sup>, A. W. Burner <sup>c</sup> and G. A. Fleming <sup>c</sup>

<sup>a</sup> Northrop Grumman Corp., One Northrop Ave., MS 9G23/GS, Hawthorne, CA 90250

<sup>b</sup> Mission Research Corp., P.O. Box 8309, Laguna Hills, CA 92626

<sup>c</sup> NASA Langley Research Center, Hampton, VA 23681-2199

## ABSTRACT

To quantify the benefits of smart materials and structures adaptive wing technology, Northrop Grumman Corp. (NGC) built and tested two 16% scale wind tunnel models (a conventional and a 'smart' model) of a fighter/attack aircraft under the DARPA/AFRL/NASA Smart Materials and Structures Development - Smart Wing Phase 1. Performance gains quantified included increased pitching moment ( $C_M$ ), increased rolling moment ( $C_l$ ) and improved pressure distribution. The benefits were obtained for hingeless, contoured trailing edge control surfaces with embedded shape memory alloy (SMA) wires and spanwise wing twist effected by SMA torque tube mechanisms, compared to conventional hinged control surfaces.

This paper presents an overview of the results from the second wind tunnel test performed at the NASA Langley Research Center's (LaRC) 16ft Transonic Dynamic Tunnel (TDT) in June 1998. Successful results obtained were: 1) 5 degrees of spanwise twist and 8-12% increase in rolling moment utilizing a single SMA torque tube, 2) 12 degrees of deflection, and 10% increase in rolling moment due to hingeless, contoured aileron, and 3) demonstration of optical techniques for measuring spanwise twist and deflected shape.

## 1. INTRODUCTION

The purpose of the Northrop Grumman Smart Wing Phase 1 program was to explore the use of integrated smart materials into an aircraft structure to provide unique capabilities resulting in significant aerodynamic performance improvements. Further, the program was to demonstrate these capabilities during wind tunnel tests at NASA LaRC 16ft TDT wind tunnel. An overall program review can be found in Reference 1.

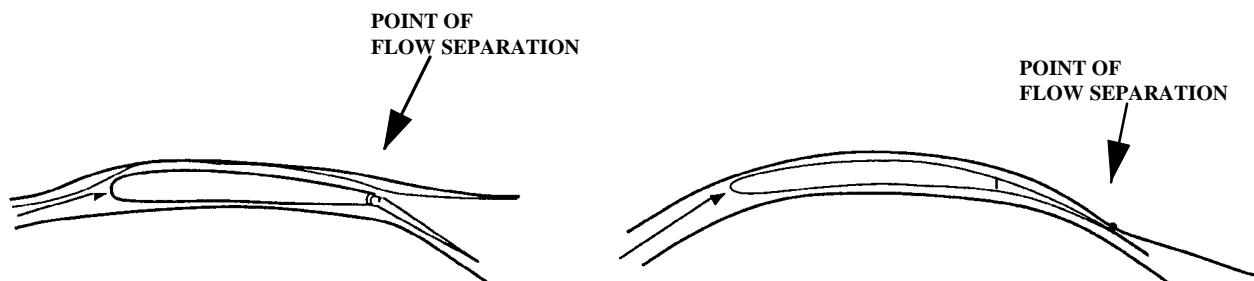


**FIGURE 1 FLOW CHARACTERISTICS OVER HINGED AND HINGELESS CONTOURED CONTROL SURFACES**

Two aerodynamic concepts were focused on, which uniquely utilized smart materials. The first was the smooth contoured trailing edge control surface. The drawback of the hinged control surface is the sharp discontinuity at the hingeline. This discontinuity can cause the flow to separate prematurely, as shown in Figure 1, causing a degradation in performance which becomes more pronounced at higher control surface deflections. The air flow with a smooth contoured control surface, in contrast, stays attached longer, significantly improving the overall pressure distribution. SMA wires were incorporated into a flexible structure on the Smart model flap and aileron to provide the smooth contoured control surface when actuated. A complete description of the SMA trailing edge control surfaces is described in Martin<sup>2</sup>. The second aerodynamic improvement concept utilized an SMA torque tube, Jardine<sup>3</sup>, to provide wing twist inboard to outboard. Increasing the local

angle of attack on the wing outboard area provides for increased lift and pitching moment. This adaptive feature would have application for take-off and landing configurations.

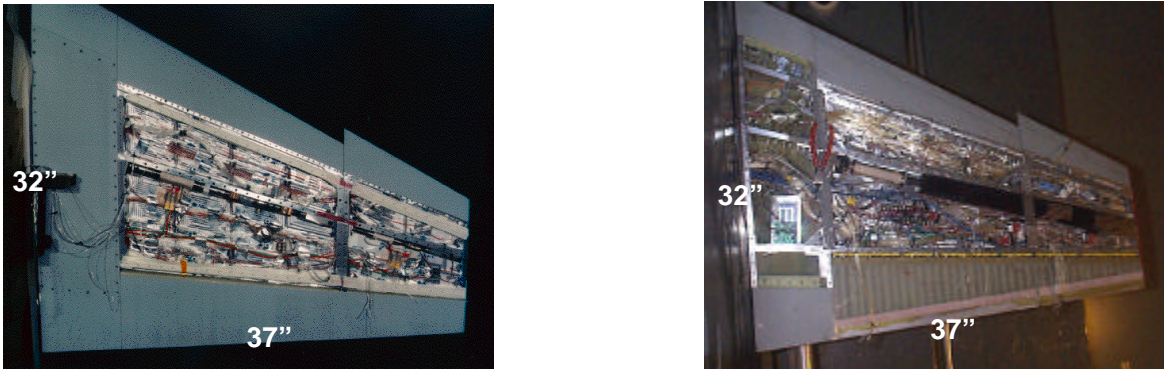


**FIGURE 2 CONVENTIONAL AND SMART WING MODELS**

Two wind tunnel models, shown in Figure 2, were tested in the NASA Langley TDT wind tunnel facility. One model was a baseline conventional fighter-type wing, utilizing standard hinged trailing edge control surfaces with a trailing edge flap and aileron. The other model was the smart wing, identical in shape and construction to the conventional wing, with the exception of SMA wire actuated flap and aileron, and a SMA torque tube. Two tests were conducted for maximum risk reduction:

- Test 1 - First demonstration of smart wing<sup>4</sup> - validating aerodynamic benefits for a preliminary proof of concept, performed in May 1996.
- Test 2 - Second iteration of integrated smart wing concept demonstration - further quantifying aerodynamic benefits and establishing technology integration payoffs/ issues, performed in June 1998.

Configuration	Deflection or Wing Twist (Deg.)	Lift $\Delta$ CL	Roll $\Delta$ CI	% Improvements	
				Lift	Roll
Flap Only (Test 1)	7.5	0.0581	0.0193	9.7%	10.2%
Flap and Aileron Combined (Test 1)	7.5	0.0916	0.0387	17.6%	17.1%
Aileron Only (Test1)	5		0.015		8.0%
Aileron Only (Test 2)	10		0.0189		10.5%
Wing Twist (Test 2)	3	0.0344	0.0193	8.0%	10.0%
	5	0.0502	0.0296	11.5%	15.6%
Wing Twist (Test 1)	1.4	0.0406	0.0218	10.0%	12.8%
Combined Aileron & Wing Twist (Test 2)	+10 ° Aileron, +4.5 ° Wing Twist	0.0567	0.031	15.3%	17.3%

**FIGURE 3 SUMMARY OF WIND TUNNEL TEST RESULTS**

Figure 3 provides a summary of notable aerodynamic improvements for the single effects of flap, aileron, and wing twist and the combined effects of flap with aileron, and wing twist with aileron for both tests. Although the focus of this paper is the results of the second test entry, it is important to delineate the accomplishments that the integration of smart materials can provide to overall aircraft aerodynamic performance. The deflection or twist is listed in degrees for each configuration including delta lift and roll aerodynamic performance improvements and provided in both absolute and percentage terms. As a general comment, it can be seen that percentage improvements of the smart technology, approached or exceeded 10 % for the single effects, and ranged between 15 and 17 % for combined effects. It should be pointed out that percentages are relative to a “safe maneuver” of 8 degrees AOA, 2g turn and a dynamic pressure of 90 lbs per square foot (~200 mph).

A 10% improvement in lift and roll performances, in more tangible practical terms, would translate to:

- a 2000 lb increase in take off gross weight (TOGW) for a typical 40,000 lb fighter attack aircraft
- an increase in steady rolling rate from 120 degrees/sec to 132 degrees/sec for the equivalent conventional and contoured aileron deflection

The Test 2 flap results, due to failure discussed in Reference 2, are an obvious table omission from Figure 3. Therefore the absence of any real flap data in Test 2 precluded a direct comparison between wind tunnel entries for this particular function. However, in all other respects, Test 2 gave encouraging results and moved the technology further forward. Test 1 represented a significant demonstration of the technology and concepts; nevertheless, some restrictions of the test set up and performance arose due to limitations of scope. Issues and factors restricting the Test 1 execution included:

- SMA wire fatigue problems at termination of control surface trailing edge
- Limited deflection capability: flap  $\pm 7.5$  degrees, aileron  $\pm 5$  degrees
- Non- uniform deflection of flap and aileron, particularly in the spanwise direction
- Maximum wing twist of 1.25 degrees, short of the 5 degree goal

All of the foregoing limitations were corrected in Test 2, which went according to plan except for a failure that limited the data collected for the SMA flap<sup>2</sup>. Figure 4 highlights the achievements, results and benefits attributed to the program Test 2 effort. Perhaps the best improvement came in the updated single torque tube design<sup>3</sup> that permitted the target 5 degree twist angle to be realized. However, across the board, all of the smart control surface concepts benefited from considerable design improvements over the configurations used in the first test. Model design enhancements unilaterally equated to higher deflection angles and improved fatigue characteristics and more uniform control surface deflections.

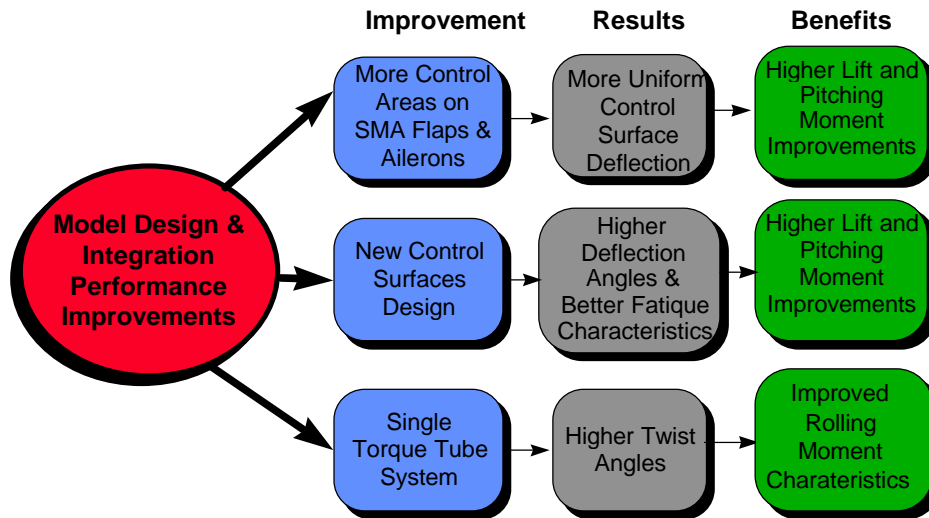


FIGURE 4. SMART WING TEST 2 OVERVIEW

## 2.1 NASA Langley 16 Foot Transonic Dynamics Tunnel

The NASA LaRC TDT<sup>5</sup> was used to test and quantify the aerodynamic performance benefits of both wind tunnel models. The TDT is a unique facility in that it is designed primarily for aeroelastic research, and validating vehicle performance for safe operation with respect to aeroelastic instability. It is important to understand that the models used for the smart wing program were not designed to study aeroelastic effects, however since their construction was similar to an actual aircraft wing, there was concern of possible dynamic effects on the models while under air loads. The TDT's test section is 16 ft. by 16 ft. and easily accommodated the test models. The facility can provide variable tunnel total pressure from near vacuum to one atmosphere from Mach numbers of 0.1 to above the speed of sound at Mach 1.2. The facility also has the unique capability of using either air or R-134A high density gas, which greatly assists in the scaling of aeroelastic models. The high density gas, however, was not required for testing on the Phase 1 program.

## 2.2 Wind Tunnel Models and Tunnel Installation

Two semi-span wing models were representative of a typical fighter-attack wing. Both wing models were identical in size, contour, and construction<sup>2</sup> similar to an actual aircraft wing with spar and rib interior construction and aluminum skins. The conventional wing model had an electrically driven, remotely actuated trailing edge flap and a manually moveable hinged aileron. The smart wing had a smooth contoured trailing edge flap<sup>2</sup> of the same size as the conventional wing. It was actuated by electrically powered SMA wires located in the upper and lower skins of the flap. The smart wing aileron also provided smooth contour and was actuated in the same manner. The smart wing also incorporated a single SMA torque tube system<sup>3</sup> close to the mid-spar which was actuated by the heating of Nichrome wire wrapped around the SMA torque tube.

Figure 5 is representative of the test installation and shows a plan view of the smart wing demonstration article as installed in the test chamber of the Langley TDT. Each model was mounted approximately three feet off the wall on a splitter plate, shown in Figure 5, which moves the model out of the wall boundary layer and toward the center of the tunnel where air flow is more uniform. Each model was firmly supported on the NASA Langley Semi-Span Turntable System which extended through the tunnel wall. The turntable provided capability for the model to be pitched through an angle of attack range of  $\pm 30$  degrees if required.

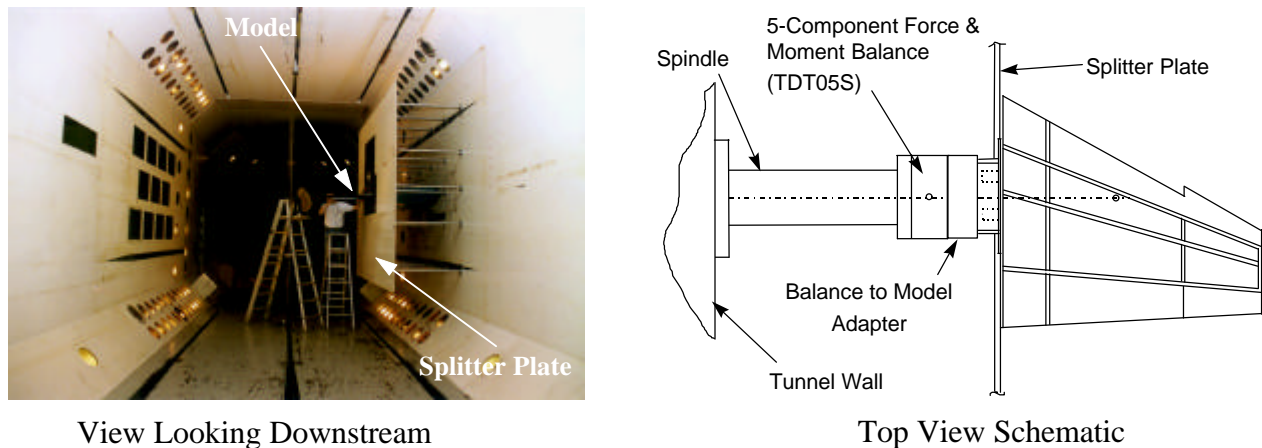


**FIGURE 5 MODEL INSTALLATION IN NASA LANGLEY 16 TDT WIND TUNNEL**

Critical set up items also depicted in Figure 5 were the spindle and balance. The spindle was necessarily rigid to provide adequate support for the model, which is cantilevered off the turntable. The spindle and balance were protected from the airflow by an enclosed fairing or “canoe”. Details of the model balance are provided in the following subsection.

## 2.3 Test Instrumentation and Monitoring

Each model was extensively instrumented during testing to record test conditions and results. The model instrumentation employed may be broadly divided into three categories:

- Aerodynamic force and moment measurement and pressure instrumentation
- Surface contour deflection and wing twist
- Safety and routine test condition monitoring

The aerodynamic monitoring was performed using NASA Langley's by TDT-05S, a five component force and moment balance capable of recording the lift and drag forces, and pitching, rolling, and yawing moments. Each of the models had four chordwise rows of static pressure taps to measure local steady state static pressure as shown in Figure 6. The pressure tubes were routed through the splitter plate and into the "canoe" fairing where they connected to a port on one of five Electronically Scanned Pressure (ESP) modules. These modules were operated and calibrated on-line by the TDT's PSI 8400 Control System.

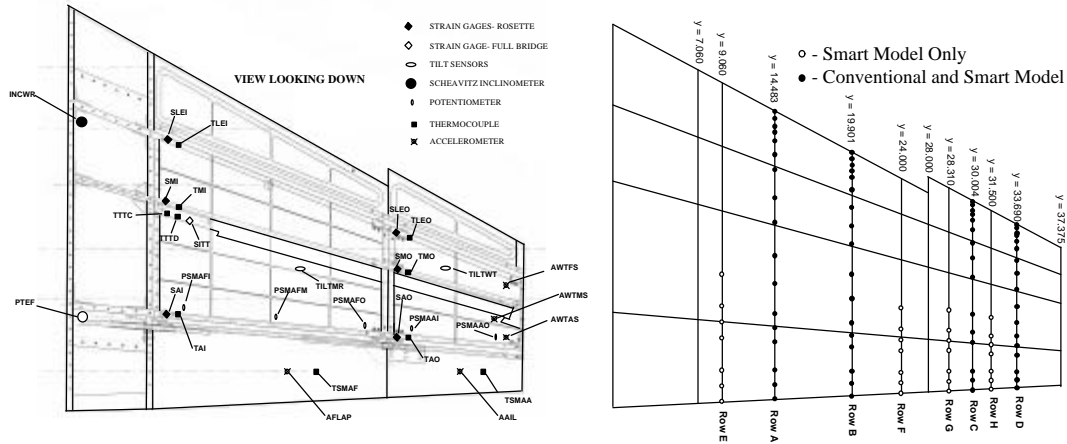


**FIGURE 6 INTERNAL INSTRUMENTATION AND STATIC PRESSURE PORT LOCATIONS**

Smart control surface contour tip deflection measurements were obtained using both internal and external methods. The external methods, however, proved to be the most reliable. Figure 7 shows the primary approaches used in determining the tip deflections.

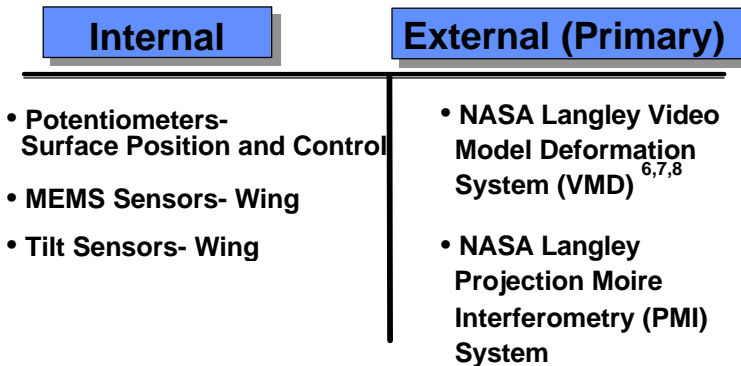


**FIGURE 7 INSTRUMENTATION SUMMARY OF CONTOUR AND WING TWIST MEASUREMENT**

An internally mounted rotary potentiometer was used to measure flap position for the conventional wing. The aileron deflection angle, though, was set manually by brackets. These brackets were prepared before testing began and were fabricated in  $\pm 5$  degrees,  $\pm 10$  degrees, and  $\pm 15$  degrees settings. The smart wing used linear potentiometers at each of the three control areas on the SMA flap and the two areas on the SMA aileron. The potentiometers attached to the tips of the SMA flap and aileron by a single wire and were located just forward of the aft spar. The attachment wire was free to move within the flap through a channel in the RTV skin. Tip deflection measurement using linear potentiometers, however, proved to be satisfactory but not optimal in terms of deflection accuracy and repeatability. The main concern was that although deflection was provided, they did not provide a measurement of the amount of curvature.

A Q-Flex inclinometer was mounted on the spindle pitch mechanism and a Scheavitz Inclinometer was mounted at the root of each model to measure the angle of attack. Other internal devices were investigated for their ability to measure wing rotation due to twisting. Among the other devices were MEMS sensors developed at Langley and tilt sensors manufactured by Advanced Orientation Systems Inc., both of which were attractive for their small size, which aided installation into the outboard wing sections. The MEMS sensors, which performed to within the required  $\pm 0.25$  degrees static accuracy, deteriorated to as high as  $\pm 5.0$  degrees under dynamic conditions. The electrolytic tilt sensors behaved well under dynamic conditions but also suffered from reliability problems with respect to discrepancies in the measured slope between positive and negative angles. The key purpose of all of the internal sensors was to provide accurate position data for the contoured surfaces and spanwise twist that could be used in wind tunnel measurements or in flight. (Developing and using sensors for real time feedback to be used for the flight control system is an extension of the previous idea that should be further pursued

on a follow on program, and all of the methods in the left hand column of Figure 7 , though lacking in maturity, should be encouraged for further development.)

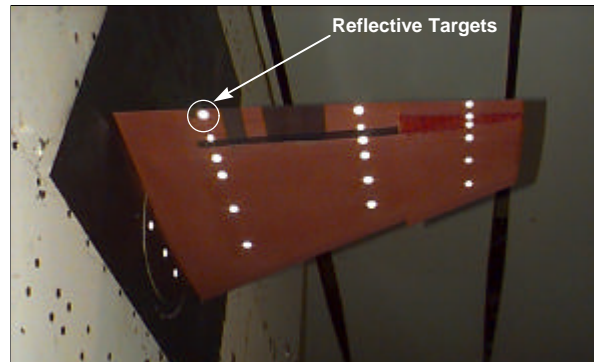


**FIGURE 8. NASA LANGLEY VIDEO MODEL DEFORMATION (VMD) SYSTEM**

External methods, on the other hand, were much more successful on the program for measuring control surface position and twist. The NASA Langley optical Video Model Deformation (VMD) system<sup>6,7</sup> was the primary system for measuring SMA flap and aileron position and wing twist. The method employs a series of small retro-reflective tape discs carefully placed at several spanwise rows as shown in Figure 8. The discs serve as targets, which when illuminated with a light generate a high-contrast image in a strategically located CCD camera. Image processing is used to automatically locate the targets. Photogrammetry is then used (after calibration) to determine the motion of the targets in the pitch plane and hence compute angular changes at the various spanwise target locations. The system is able to provide angular deflection in "near real-time" with updates in angle approximately a few seconds after triggering.

Projection Moiré Interferometry (PMI) was a second external optical diagnostic technique used to measure wing surface shape and deformation. The PMI system used an infrared, pulsed laser to project a series of equispaced, parallel lines onto the lower surface of the model. Images of the projected grid lines were captured using a CCD camera and frame grabber in reference (wind-off) and wind-on conditions. Image processing techniques were then used to reconstruct the model surface shape and/or deformation under aerodynamic load. Figure 8 shows PMI-measured quantitative wing surface shape measurements for the smart wing in non-actuated and torque-tube-actuated conditions. The PMI measurements were spatially continuous at a resolution of 0.055 in. per pixel (1.4mm per pixel), far exceeding that of the VMD system. However, at its current state of development for wind-tunnel testing, PMI does not possess the high degree of accuracy demonstrated by VMD, and quantitative real-time output is not possible.

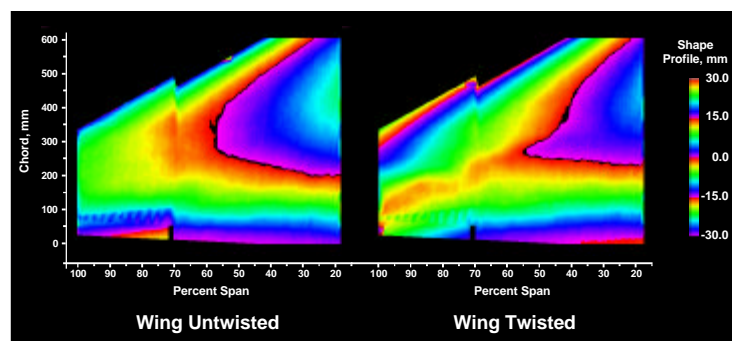


**FIGURE 9 NASA LANGLEY PROJECTION MOIRÉ INTERFEROMETRY (PMI) SYSTEM**

The third category of instrumentation used during the wind tunnel testing relates to instruments used to monitor model and facility safety. Among the sensors used to monitor the model were strain gages, accelerometers and thermocouples. The location of these sensors is shown in Figure 6. The three accelerometers at the wing tip were installed to monitor model dynamics. The strain gauge rosettes, mounted inboard and outboard on each of the three wing spars, provided real time model dynamics and structural load monitoring. Thermocouples were installed on the SMA torque tube, naturally, to monitor its temperature. They were also co-located with the strain gages to provide temperature compensation for the strain, if necessary, and determine the effect on the internal temperature through out the model due to torque tube actuation.

## 2. 4 Program Test Sequence and Conditions

A flutter clearance run was made at the start of the test for each of the two models as a safety precaution to ensure model dynamic stability prior to recording any actual wing model performance data. The model was taken slowly to increasing dynamic pressures and Mach numbers, for flutter clearance, and angle of attack varied between 0 and 10 degrees. The reason for doing this was to clear the test envelope and verify that the model behaved dynamically as expected in the test range.

The models were tested at two different constant tunnel total pressures of one atmosphere (sea level or 2200 psf) and 0.5 atmosphere (17,000 ft altitude or 1100 psf). Tunnel freestream dynamic pressures were set at 60, 90, or 120 psf. This would correspond to Mach numbers of 0.2, 0.25, and 0.29 respectively at one atmosphere and 0.3, 0.36, and 0.4 respectively at 1100 psf tunnel total pressure. Data was recorded at specified, fixed angles of attack (AOA) starting at -4 degrees and increasing up to +16 degrees in fixed increments of 2 degrees except near the 0 degree AOA point, where the increment was 1 degree. Run polars, plots of aerodynamic coefficients ( $C_L$ ,  $C_M$ , etc.) versus AOA, were generated at various total pressures, Mach numbers and fixed wing twist / control surface configurations. The means of measurement was as follows:

- TE flap deflection angle on conventional model was set with an electric motor and calibrated with a rotary potentiometer
- Aileron deflection angle was set with fixed brackets
- Smart wing SMA trailing edge deflection and wing twist measured optically (described above).

## 3. TEST RESULTS

A top level discussion of the wind tunnel test results was presented in the introduction. This section reviews in more detail each individual function tested. The wind tunnel results are discussed by adaptive concept, and in general, results for each configuration on the conventional wing are compared directly to the equivalent configuration on the smart wing. This grouping of topics helps clarify the data presentation as compared to a chronological form. Hence, subsections are structured into:

- Baseline repeatability
- Wing twist
- Aileron performance
- Combined effectors

### 3.1 Baseline Repeatability

Data was first compared for the baseline configurations, i.e., all control surfaces at a neutral or undeflected state between the conventional wing and smart wing. This was to ensure that the two models were identical in shape and to verify proper installation. Baseline repeatability data shown in Figure 10 (Mach = 0.25 and dynamic pressure of 90 psf) shows plots of lift, pitch, and rolling moment coefficient versus angle of attack. The data plots shows very good comparisons between the conventional and smart wing, giving confidence that the incremental data obtained from subsequent tests to establish performance improvements for the smart wing would be accurate.

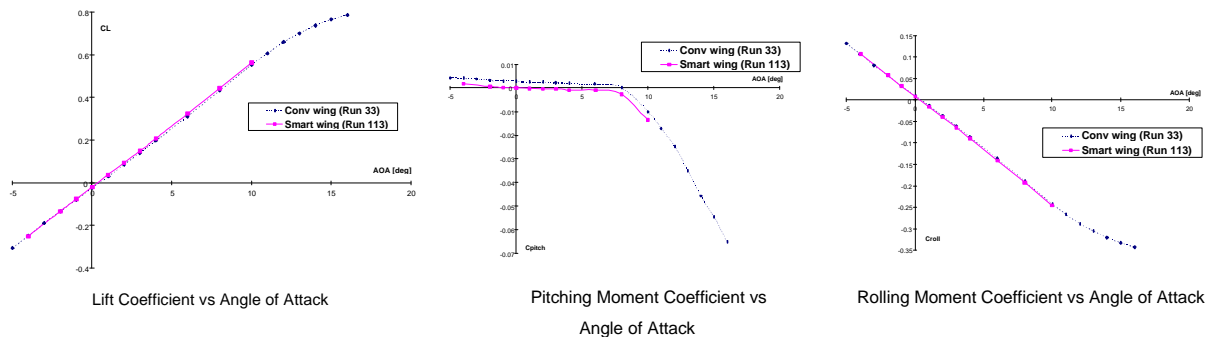
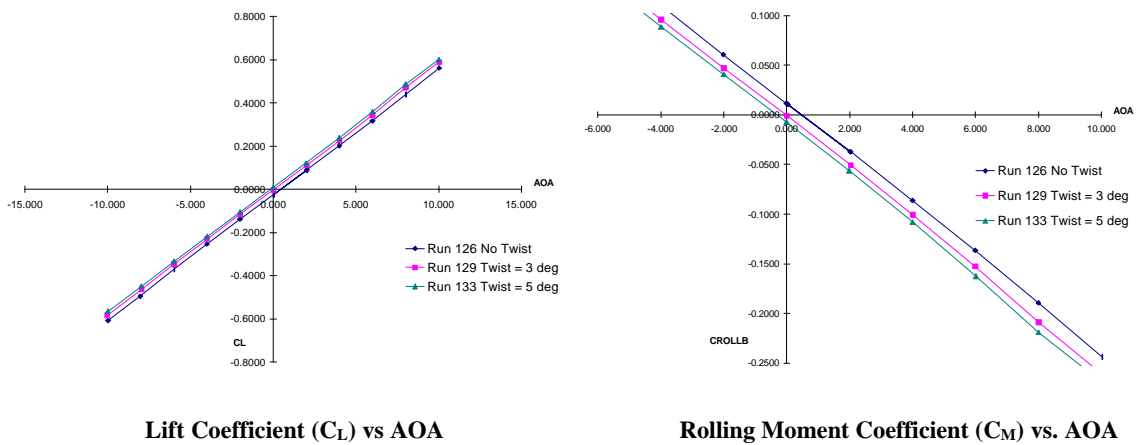


FIGURE 10 BASELINE REPEATABILITY - TEST 2 (Q = 90 PSF, MACH = 0.25)

### 3.2 Wing Twist

One of the primary objectives of the second test entry was to increase spanwise wing twist from +1.25 degrees in Test 1, to +5 degrees. This objective was accomplished and plots of the lift and rolling versus angle of attack for the smart wing untwisted and twisted at 3° and 5° are shown in Figure 11. These incremental improvements, however, were relatively not as large as obtained from the first entry. A 1.25° twist provided an approximate 12.8% rolling moment improvement at 8 degrees of angle of attack while for test entry 2, a 3 degree wing twist provided a 10% rolling moment increase at the same angle. Closer examination revealed that for the first entry, the inboard section of the wing was actually twisted more than during the second wind tunnel entry. Briefly, for the first entry a tandem system of SMA torque tubes<sup>3</sup> was used, one from the inboard rib to the mid rib and another from the mid rib to the outboard rib. In test entry 2, only one torque tube with its attachments connecting the inboard rib to the outboard rib was used. This approach provided significantly more twist at the outboard wing tip than the first entry but not on inboard side of the wing where there is greater amount of wing area. Inboard rib to mid rib accounts for 73% of the wing area for this particular configuration. Figure 12 shows the amount of twist along the length of the wing reflecting the inboard twist and the differences between Test 1 and Test 2. Future work might concentrate resources on the inboard section of the wing installation area.



**FIGURE 11. WING TWIST EFFECTS - TEST 2**  
**(FLAP = 0 DEGREES, Q = 90 PSF, MACH = 0.25)**

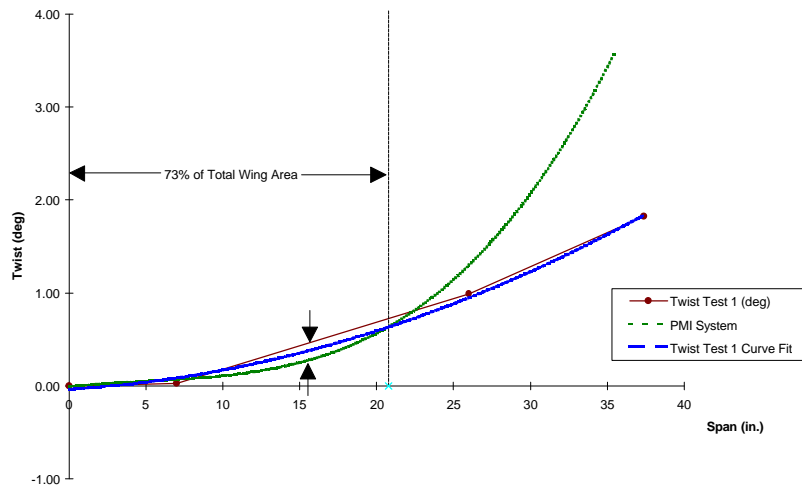


**FIGURE 12. SPANWISE TWIST DISTRIBUTION DUE TO SMA TORQUE TUBE**

### 3.3 Aileron Performance

The performance benefits afforded by the SMA actuated flap and aileron, versus a hinged configuration, is perhaps, one of the most critical results and achievements of the smart wing phase 1 program. Although the SMA flap failed<sup>1\*</sup> during the second entry, the aileron demonstrated the performance gains of using a smooth contoured control surface. Figure 13 shows the improved pressure distribution on the contoured aileron (dark area) versus a hinged aileron (light area) with reduced flow separation at the trailing edge. A superior design addressed the first test limitations which limited maximum deflection and uniform deflection along the span. The new design increased deflection from 5 to 10 degrees and provided for a more uniform deflection. The benefits of the contoured aileron over the hinged aileron at 10 degrees of deflection are shown in Figure 14. The 10.5% improvement, shown in Figure 14, is a 2.5% improvement above the first entry results at the same test conditions.

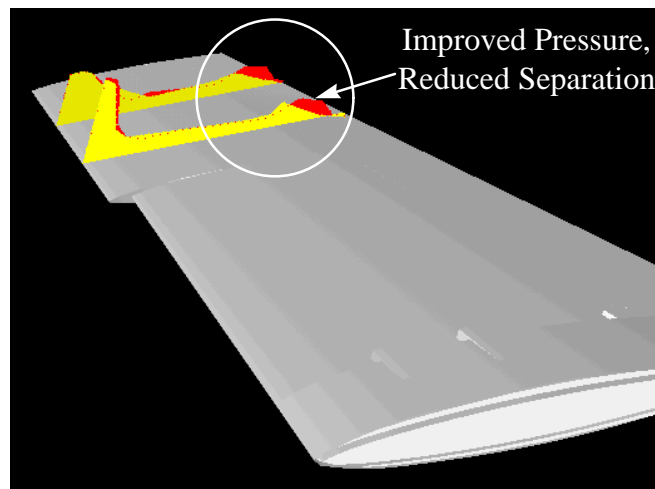


**FIGURE 13 AILERON EFFECTIVENESS, PRESSURE PLOT (RUN 41 vs. 116, Q = 90, AOA = 6)**

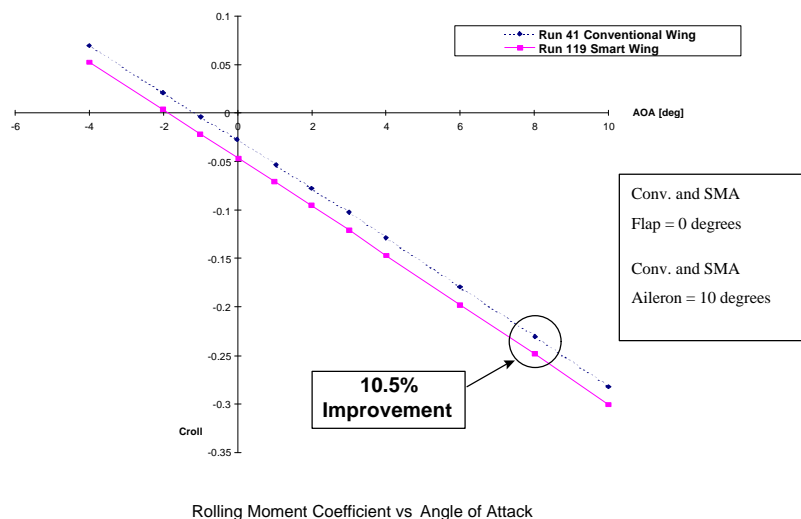


**FIGURE 14. AILERON EFFECTIVENESS - 10 DEGREES DEFLECTION - TEST 2 (Q = 90 PSF, MACH = 0.25)**

<sup>1\*</sup> Detailed explanation is given in Reference 2. From Test 1, flap performance showed substantial benefits<sup>1</sup> despite lower deflection angles and non-uniform distribution

An alternative method of visualizing the aileron effectiveness is illustrated in Figure 15. Here the rolling moment coefficient due to aileron deflection is plotted for different angle of attack, namely at  $\alpha = 6, 8,$  and  $10$  degrees. Two important features are shown on this graphic. First, at zero degrees deflection, the rolling moments are very close which would indirectly verify the consistency between the models. The second is the increase in performance improvement with increasing control surface deflection angle. This shows that the separation reduction the contoured aileron provides results in an improved lifting surface and a lower deflection angle to obtain the same lift as a conventional aileron.

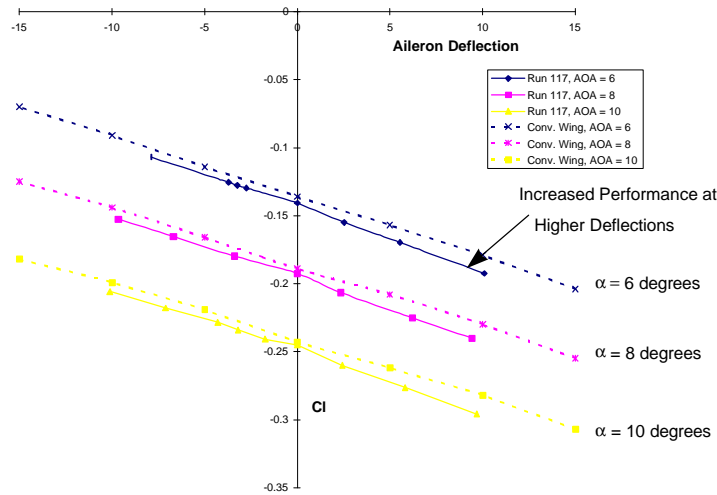


**FIGURE 15. AILERON EFFECTIVENESS - ALPHA VARIATION**  
( $Q = 90$  PSF,  $MACH = 0.25$ )

### 3.4 Combined Performance

It is important to appreciate that in all of the adaptive effects discussed so far, it is unlikely that any one of them will be used exclusively in isolation for a complete mission. There will be many instances where effects will be combined such as during take-off and landing where the flap and aileron will be actuated simultaneously, or a combination of wing twist with aileron might be used. Test 2 examined the combined effects of aileron and wing twist on rolling moment. Figure 16 demonstrates a substantial improvement of 17% (at 8 degrees angle of attack) when both twist and contoured aileron are used in unison compared to a conventional aileron alone. This further demonstrates the benefits of using smart control surfaces.

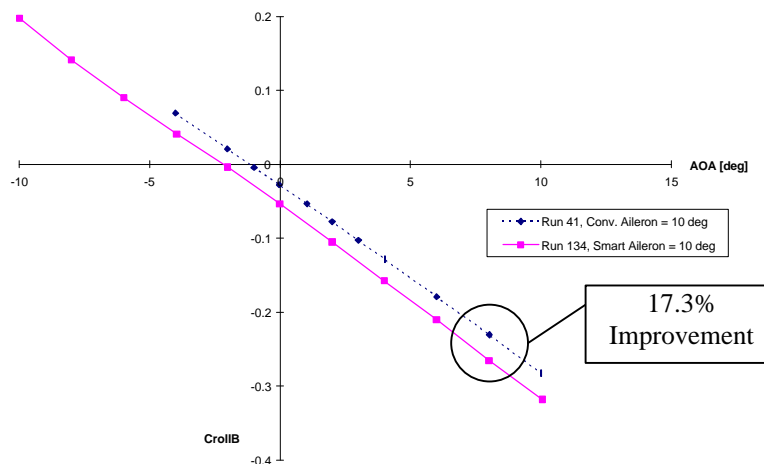


**FIGURE 16. ROLLING MOMENT INCREASE FOR COMBINED WING TWIST AND SMART AILERON DEFLECTION**

#### 4. CONCLUSIONS AND FUTURE PLANS

The results of the second entry of the Smart Wing Phase 1 Test Program demonstrated further improvements in aerodynamic performance. Design limitations of scope and integration issues from the first entry were successfully addressed. The following benefits were quantified through the use of improved SMA actuated smooth contoured aileron and increased wing twist via an SMA torque tube:

1. Further improvements in rolling moment as compared to a conventional aileron.
2. Further improvements in overall pressure distributions.
3. Increased wing twist angles from  $1.25^\circ$  in the first entry to  $5^\circ$  in the second entry

Phase 2 of the Smart Wing Program will address:

- Increased bandwidth or actuation speed of the control surfaces
- Structural integration issues with increased loading of the control surfaces up to and including transonic speeds
- Improved control laws for actuation
- Internal instrumentation for control surface curvature and deflection measurement

Two wind tunnel tests, one in October 1999 and the other in September 2000, are planned using a 30% scale NGC Uninhabited Combat Air Vehicle (UCAV) design.

#### 5. ACKNOWLEDGEMENTS

This work was supported under the DARPA / AFRL / NASA Smart Materials and Structures Development- Smart Wing contract, F33615-93-C-3202, initiated by Dr. Bob Crowe, and currently managed by Dr. Ephraim Garcia. The authors would like to thank the Air Force Research Laboratory program monitors Dr. George Sendeckyj, Mr. Terry Harris, and Maj. Brian Sanders. We would also extend appreciation to Ms. Anna-Marie R. McGowan, Ms. Renee Lake and other members of the NASA Langley TDT facility team for all their support during all phases of the test program.

#### 6. REFERENCES

1. J. N. Kudva et al., "Overview of DARPA / AFRL / NASA Smart Wing Program", SPIE Proceedings Vol. 3674, No. 3674-26, March 1-4 1999, Newport Beach, CA.
2. C. A. Martin, J. Bartley-Cho, J. Flanagan, B. F. Carpenter, "Design and Fabrication of Smart Wing Model and SMA Control Surfaces", SPIE Proceedings Vol. 3674, No. 3674-27, March 1-4 1999, Newport Beach, CA
3. A. P. Jardine, J. Bartley-Cho, J. Flanagan, "Improved Design and Performance of the SMA Torque Tube for the DARPA Smart Wing Program", SPIE Proceedings Vol. 3674-28, March 1-4 1999, Newport Beach, CA
4. L. B. Scherer, C. A. Martin, K. Appa, J. N. Kudva, M. N. West, "Smart wing test results", SPIE Proceedings Vol. 3044, No. 3044-02, March 1997
5. "The NASA Langley Transonic Dynamics Tunnel", NASA LWP-799, September 1969
6. A. W. Burner, "Model Deformation Measurements at NASA Langley Research Center", AGARD CP 601 (Presented at the 81<sup>st</sup> Fluid Dynamics Panel Symposium on Advanced Aerodynamics Measurement Technology, 22-25 September, 1997, Seattle, Washington) pp. 34-1 to 34-9, May 1998
7. J. H. Bell and A. W. Burner, "Data Fusion in Wind Tunnel Testing; Combined Pressure Paint and Model Deformation Measurements", Paper No. AIAA 98-2500, Presented at the 20<sup>th</sup> AIAA Advanced Measurement and Ground Testing Technology Conference June 15-18, 1998, Albuquerque, NM
8. G. A. Fleming, A. W. Burner, "Deformation Measurements of Smart Aerodynamic Surfaces", Paper to be Presented at SPIE International Symposium on Optical Science, Engineering and Instrumentation, July 18-23, 1999, Denver, CO